Available online at www.sciencedirect.com
ScienceDirect
Tetrahedron 64 (2008) 3760–3771
Tetrahedron
www.elsevier.com/locate/tet

Liquid crystal dimers derived from naturally occurring chiral moieties: synthesis and characterization

Channabasaveshwar V. Yelamaggad*, Govindaswamy Shanker

Centre for Liquid Crystal Research, Jalahalli, Bangalore 560013, India

Received 30 November 2007; received in revised form 5 February 2008; accepted 6 February 2008
Available online 8 February 2008

Abstract

Naturally occurring cholesterol and α-chloroalkanoyl units derived from natural α-amino acids (L-valine, L-leucine, and L-isoleucine) have been utilized to prepare three different series of nonsymmetric liquid crystal dimers. Tolane (diphenylacetylene), which is known to possess several promising structural features, has been chosen as the other mesogenic segment to covalently tether with cholesterol through a flexible spacer. In each series, the terminal α-chloro ester group attached to the tolane unit is kept constant, while the length and parity of the spacer have been varied; specifically, three dimers comprising even-parity spacer of varying length, and one compound with an odd-parity spacer constituted a series. The phase behavior of these dimers has been ascertained mainly by polarizing microscopic and calorimetric studies. Except one, all the 11 dimers display enantiotropic mesomorphism. Within the series, clearing temperatures exhibit a dramatic odd–even effect wherein the even-parity dimers possess higher values. In general, the dimers comprising α-chloro ester group derived from L-valine and L-leucine stabilize chiral nematic and/or smectic phase/s, while the compounds with terminal group resulting from L-isoleucine show twist grain boundary phase additionally; this implies that the nature of the α-chloro ester group influences the phase behavior. Notably, an odd-parity dimer with an α-chloro ester group derived from L-valine exhibits a transition from an intercalated smectic A phase to a monolayer (unknown) smectic phase, as evidenced by optical, calorimetric, and X-ray diffraction studies. As representative case, a dimer has been screened for antimicrobial activity by disc diffusion method; a notable activity has been found against some microbes.

1. Introduction

Liquid crystal (LC) phases (mesophases) are fascinating orientationally ordered fluids formed by the self-assembly of shape-anisotropic molecules, so called mesogens.[1] The chiral LC phases generated by optically active mesogens or by doping the mesophase with a suitable chiral dopant are even more fascinating as they possess a dizzying array of special properties and structures that are promising from both fundamental science and application view points.[2–6] For example, the frustrated fluid phases such as blue phases (BPs)[2,3b] and twist grain boundary (TGB) phases[2,3] are of fundamental scientific curiosity, while the helical structures of the chiral nematic (N*) or chiral smectic C (SmC*) have been recognized for their use in thermochromic[4] and electro-optic devices, respectively.[5] Besides, electroclinic property of the orthogonal layered phase, the chiral smectic A (SmA) phase holds a great promise in spatial light modulation applications.[6] However, the properties of these chiral mesophases fundamentally depend on the chirality of the constituent molecules, which in turn critically depends on the nature of the chiral segment/s they possess.[2,3] Likewise, the origin of a particular chiral LC phase in preference to other or their occurrence in a phase sequence is also speculated to be evolving from the molecular chirality of the constituent mesogens. In other words, by the rational design of chiral LCs incorporating appropriate chiral building block/s, the features of the chiral mesophases can be modified; of course, not all the optically active LC materials prepared based on such directed molecular design exhibit the speculated property.

* Corresponding author.
E-mail address: yelamaggad@yahoo.com (C.V. Yelamaggad).

0040-4020/$ - see front matter © 2008 Elsevier Ltd. All rights reserved.
doi:10.1016/j.tet.2008.02.013

The chiral moieties employed in building mesogens are generally chosen from the chiral pool, the readily available natural products or their modified forms, and synthetic products.[2,7,8] The former approach appear to be more appropriate given the fact that the natural products, needless to say, are structurally diverse and economically feasible. Besides, naturally occurring moieties or their derivatives are well known to induce interesting features in the systems where they are used. For example, chiral polar terminal chains, the α-chloroalkanoyl units, derived from α-amino acids viz., L-valine, L-leucine, and L-isoleucine have been evidenced to be suitable for stabilizing wide thermal range ferroelectric LC (SmC*) phase associated with high spontaneous polarization (Ps) and low rotational viscosity.[7–12] The cause for the high Ps in these systems is attributed to the presence of α-chloro ester group that induces a large lateral overall molecular dipole moment.[12] In addition, the materials possessing such chiral moiety are known to exhibit polymesomorphic sequences involving N*, SmC*, SmA phases as well as highly ordered smectic phases;[9] some of them have also shown the frustrated (BP and TGB) phases.[7e,9b,10,11] Likewise, a variety of steroids have been used to generate chiral mesophases,[13] but only cholesterol has been incorporated extensively as an important building block [13,14] owing to its rigid molecular structure possessing eight chiral centers. In fact, the first example of a thermotropic LC is derived from cholesterol, the cholesteryl benzoate.[15] Hitherto, well over 3000 cholesterol-containing compounds falling under the category of monomers,[13–15] oligomers,[16–26] and polymers[27] have been reported; indeed, the vast majority of them are the low molar mass systems, in particular the monomers.[13,14]

The accumulated experimental results clearly reveal the ability of cholesterol in generating mesomorphism in its various derivatives several of which possess remarkable phase sequences. This is especially notable in the case of optically active nonsymmetric dimers formed by covalently interlinking cholesteryl ester unit axially with different conventional aromatic mesogens containing Schiff's base,[18] salicylaldimine,[19] stilbene,[20] azo,[21] or biphenyl,[22] tolane,[23,24] diphenylbutadiene,[25] bent-core[26] units through a flexible spacer. For example, they exhibit several kinds of frustrated phases including a rarely found incommensurate smectic A (SmA_{ic}) phase;[18a] in fact, this SmA_{ic} phase exists in an unusual phase sequence appearing at the temperatures above as well as below the reentrant SmC* phase. Besides, some of these molecular systems stabilize technologically important SmA, SmC*, and N* phase over a wide thermal range.[18–26] In the context of stabilizing the frustrated and/or other chiral mesophases, our group[23] and Jin et al.[24] have been able to recognize that the tolane (diphenylacetylene) core, being nearly rigid with a little conformation deviation,[28] is highly promising. For instance, upon tethering achiral tolane entity to cholesterol unit through a pentamethylene (6-oxyhexanoyl) spacer, the N* phase of the resultant dimers is stabilized over a wide thermal range;[23a,b] on the other hand, when chiral tolane segment is used instead of the achiral one, the SmA phase (showing electroclinic effect) is stabilized.[23c,d] Remarkably, a dimer made of cholesterol and 4-*n*-hexyloxytolane moieties interlinked through an 6-oxyhexanoyl spacer displays a reentrant TGBA (comprising blocks of SmA) phase besides TGBC* phase, where the slabs of the mesogens have a local SmC* structure.[23e,24] Moreover, the tolane as an anisometric segment, is reasonably stable to heat and moisture and hence, all the cholesterol-based dimers featuring this core show highly reproducible mesomorphism. Another prominent aspect is that the tolane moiety has been considered in designing bioactive molecular systems in recent times.[29] Therefore, it seemed interesting to us to continue to work on nonsymmetric dimers composed of cholesteryl ester and tolane mesogenic segments; besides, owing to the several remarkable features of the α-chloroalkanoyl units derived from α-amino acids as discussed above, we intend to incorporate them in the dimeric molecular design. Precisely, in order to further our understanding of the structure–property correlations of cholesterol-based dimers composed of tolane entity, and to evaluate the influence of different α-chloroalkanoyl tails on the overall phase behavior, we designed and prepared three series of dimers. In each series, a particular type of chiral tail derived either from L-valine or L-leucine or L-isoleucine and four different spacers, namely, trimethylene (4-oxybutanoyl), tetramethylene (5-oxypentanoyl), pentamethylene (6-oxyhexanoyl), and heptamethylene (8-oxyoctanoyl) have been used. The acronyms used to denote these three series of dimers are **TDV-*n***, **TDL-*n***, and **TDI-*n***, where **T**, **D**, **V**, **L**, and **I** refer to **T**olane, **D**imer, **V**aline, **L**eucine, and **I**soleucine, respectively; ***n*** signifies the number of methylene units in the flexible spacer.

2. Synthesis and molecular structural characterization

The proposed dimers were prepared by the synthetic routes shown in Schemes 1 and 2. The requisite optically pure 2-chloroalkanoic acids **1a**, **1b**, and **1c** were prepared starting from the corresponding α-amino acids L-valine, L-leucine, and L-isoleucine according to a reported procedure;[30] given the fact that this reaction involves a double inversion process where the partial racemization occurs, only the fraction (colorless oil) collected in the temperature range of 75–77 °C (at 10 mm) was used. These acids were converted to the corresponding acyl chlorides **2a–c** by treating with oxalyl chloride

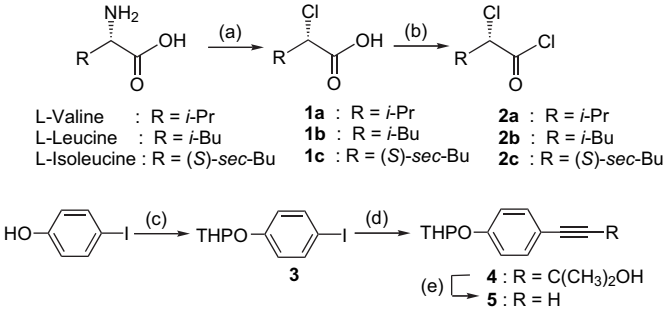

Scheme 1. Reagents and conditions: (a) $NaNO_2$, 6 N HCl, −3 to 0 °C (50–55%); (b) $(COCl)_2$, rt, 4 h (quantitative); (c) 3,4-dihydro-2*H*-pyran, PTSA, CH_2Cl_2, 2 h (82%); (d) 2-methylbut-3-yn-2-ol, CuI, Ph_3P, $(Ph_3P)_2PdCl_2$, THF, NEt_3, 85 °C, 12 h (88%); (e) KOH, toluene, reflux, 1 h (60%).

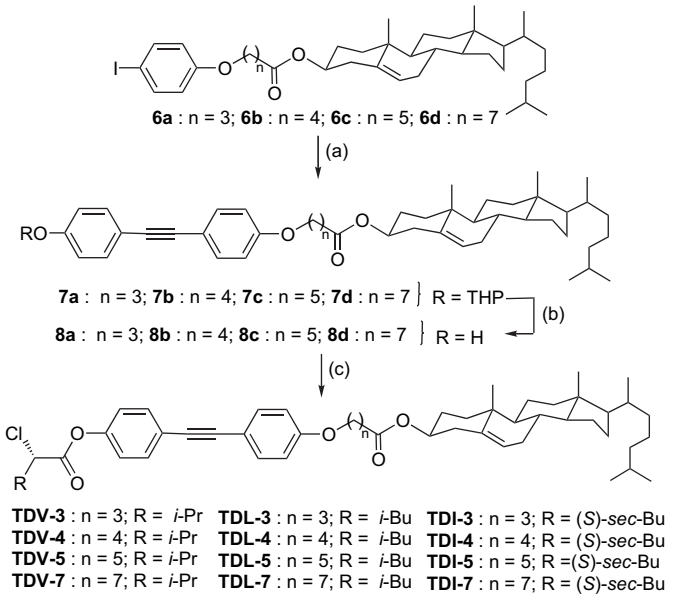

Scheme 2. Reagents and conditions: (a) **5**, CuI, Ph_3P, $(Ph_3P)_2PdCl_2$, THF, NEt_3, 85 °C, 12 h (68–72%); (b) PTSA, CH_3OH, THF, rt, 30 min (75–80%); (c) **2a–c**, pyridine, THF, 0 °C to rt, 12 h, (75–80%).

just prior to use. Next, 2-(4-ethynylphenoxy)-tetrahydro-2*H*-pyran (**5**) was prepared in three steps starting from 4-iodophenol.[17a–c] The phenol group was first protected as the THP ether to get compound **3**; palladium-catalyzed Sonogashira cross-coupling of this intermediate with 2-methylbut-3-yn-2-ol yielded protected acetylene **4**, which was subjected to a deprotection reaction to remove the acetylene protected group selectively to generate the free acetylene **5** as shown in Scheme 1.

The coupling of cholesteryl ω-(4-iodophenoxy)-alkanoates[23f] (**6a–d**) with acetylene **5** using Sonogashira conditions gave dimeric THP ethers **7a–d**, which on deprotection using PTSA in a mixture of solvents viz., CH_3OH–THF furnished the functionalized dimers **8a–d**.[17a] Finally, the esterification of phenols **8a–d** with appropriate acyl chlorides **2a–c** in the presence of a mild base (pyridine) gave the target dimers in reasonably good yields as shown in Scheme 2. The molecular structure of all the intermediates and final products was ascertained using a combination of spectral and elemental analyses (see Supplementary data).

3. Result and discussion

3.1. Evaluation of mesomorphism

The thermal behavior for each of these nonsymmetric dimers belonging to three different series was ascertained using polarizing optical microscope (POM), differential scanning calorimeter (DSC), and X-ray diffraction (XRD). The sample placed between a clean untreated glass slide and a cover slip was used for the POM study; for confirmation of assignments, two differently surface-coated slides, one treated for homogeneous alignment, the other for homeotropic alignment of the mesogens were used. The endothermic and exothermic peak temperatures obtained in DSC thermograms due to phase transitions during the first heating and cooling cycles (at a rate of 5 °C/min), respectively, were in agreement with those of the optical experiments. Of course, when the thermal signatures were not found in DSC traces, the transition temperatures are taken from the microscopic observations; the results of these investigations are shown in Table 1. In the following section, the details of these studies with analysis of the results are presented.

In general, with the exception of a dimer viz., **TDL-4**, all the members are enantiotropic mesogens. As can be seen, the dimers **TDV-3** and **TDV-5** belonging to **TDV-*n*** series, where the α-chloroalkanoyl tail they possess is derived from L-valine, display an identical enantiotropic dimesomorphic sequence. On cooling isotropic phase, they show a focal-conic texture (Fig. 1a), which on slight mechanical shear give a Grandjean planar (with oily streak, see Fig. 1b) texture typical of the N* phase.[31] Upon cooling the unperturbed sample further, multidomains begin to appear that rapidly coalesce to give a pattern consisting of focal-conic fan and pseudoisotropic textures, a diagnostic feature of the orthogonal SmA phase.[31] The occurrence of this phase was confirmed by the observation of focal-conic texture in slides treated for planar

Table 1
Phase transition temperatures[a] (°C) and enthalpies [kJ mol^{-1}] of the dimesogens

Dimers	Heating/cooling
TDV-3	Cr 117.5 [21.6] SmA 191[b] N* 194.2 [0.7] I
	I 189.3 [0.4] N* 186[b] SmA 104.9 [1.6] Cr
TDV-4	Cr 116.3 [46.1] SmA 131.8 [3.3] I
	I 131 [3.2] SmA 113.7 [2.2] SmX 68.7 [13.4] Cr
TDV-5	Cr 117.6 [18.6] SmA 167.7 [2.1] N* 172.2 [2.4] I
	I 170.4 [2.4] N* 165.5 [2.1] SmA 85.7 [14] Cr
TDV-7	Cr 127.5 [25.7] SmA 153.1 [8.3] I
	I 148.3 [5.6] SmA 58.6 [15.4] Cr
TDL-3	Cr 159.8 [15.3] SmA 198.6 [0.8] N* 208.5 [2.8] I
	I 198.4 [2.4] N* 187.3 [0.8] SmA 136.2 [15.7] Cr
TDL-4	Cr_1 123.2 [2.3] Cr_2 143.1 [19.6] I
	I 135.4 [0.9] N* 109.1 [19] Cr
TDL-5	Cr 142.5 [19.6] SmA 168.8[b] N* 169.4 [1.5] I
	I 166.5 [1.5] N* 165.3[b] SmA 119.1 [16.3] Cr
TDL-7	Cr 132.0 [12.5] SmA 164.4 [3.9] N* 170.6 [3.3] I
	I 169.7 [3.2] N* 163.1 [3.4] SmA 85.4 [5.5] Cr
TDI-3	Cr 160.0 [29.8] SmA 186.4[b]–TGB[c]–N* 196.4 [1.3] I
	I 193.5 [1.3] N* 183[b]–TGB[c]–SmA 83.6 [3.9] Cr
TDI-4	Cr 119.6 [28.6] SmA 124.8[b]–TGB[c]–N* 138.6 [1.1] I
	I 136.5 [1.1] N* 122.5[b]–TGB[c]–SmA 68.7 [2.7] Cr
TDI-5	Cr 119.7 [24.4] SmA 155.4 [4][d]–TGB[c]–N* 163.3 [3.1] I
	I 161.9 [3.1] N* 153.9. [3.4][d]–TGB[c]–SmA 55.2 [3.9] Cr
TDI-7	Cr 127.5 [34.3] SmA 155.1 [1.6][d]–TGB[c]–N* 178.6 [3.4] I
	I 177.9 [3.4] N* 153.1. [1.2][d]–TGB[c]–SmA 90.7 [13.9] Cr

Phase identified are abbreviated as Cr: crystals; N*: chiral nematic; SmA: smectic A phase; TGB: twist grain boundary phase with either SmA or SmC blocks; SmX: unknown smectic phase; I: isotropic liquid state.

[a] Peak temperatures in the DSC thermograms obtained during the first heating and cooling cycles at 5 °C/min.

[b] The phase transition was observed under POM; it was too weak to be detected by DSC.

[c] A transient phase observed under POM.

[d] The enthalpy (ΔH) value represents the combined enthalpy for both SmA–TGB and TGB–N* transition.

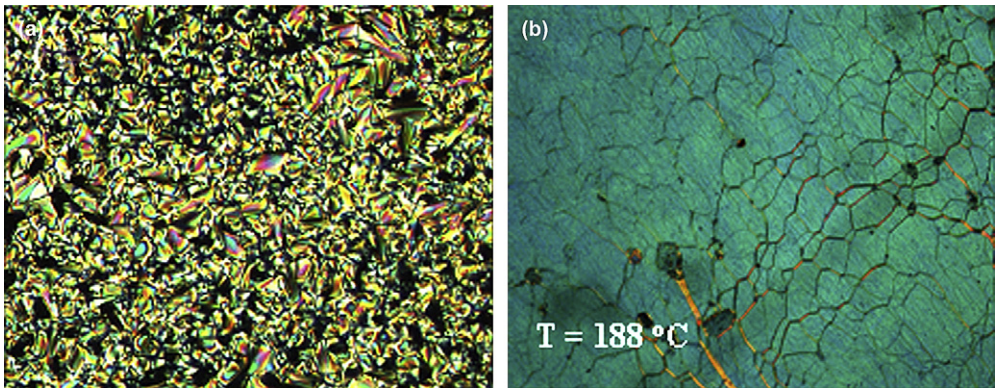

Figure 1. Photomicrographs showing the focal-conic (a) and planar (b) textures of the N* phase observed for the dimer **TDV-3**. Note that the latter texture is obtained on applying mechanical stress to the former.

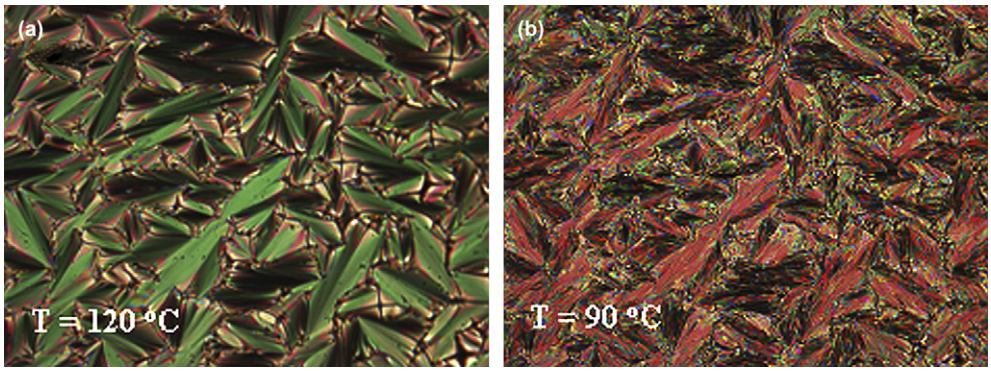

Figure 2. Microphotographs of the textures obtained for the homogeneously aligned SmA (a) and SmX (b) phases of the dimer **TDV-4**.

orientation and a dark field of view in slides treated for homeotropic orientation.

Surprisingly, the N* phase gets extinguished in other two members of the series viz., **TDV-4** and **TDV-7** as they were ascertained to display an enantiotropic SmA behavior; however, the former dimer having an odd-parity (5-oxypentanoyl; C_5) spacer stabilizes an additional metastable mesophase, hereafter referred to as SmX phase. On cooling the isotropic liquid of the samples placed between a pair of ordinary glass substrates, exhibit SmA phase with typical textures. On further cooling, the dimer **TDV-7** transforms into a crystal phase, whereas **TDV-4** shows a transition into SmX phase before it crystallizes. When the SmX phase is obtained by cooling of the preceding focal-conic texture (Fig. 2a) of the SmA phase, it showed a sort of broken focal-conic like pattern as shown in Figure 2b.

On the other hand, if it is allowed to grow from the homeotropic regions of the SmA phase, a poorly defined texture was obtained, see Figure 3a. The DSC thermograms obtained for the two successive heating and cooling cycles at a rate of 5 °C/min are shown in Figure 3b where a prominent signature due to the SmA–SmX transition can be seen; it may also be noted that the phase transitions are reproducible signifying the thermal stability of the dimer.

Powder XRD measurements using Cu Kα radiations (λ=1.5418 Å) were carried out to know the precise molecular organization in both SmA and SmX phases. The dimer **TDV-4** was filled into a Lindemann capillary tube in the isotropic phase and then both the ends of tube were flame sealed. The XRD patterns obtained in the SmA and SmX phases at 125 °C and 90 °C, respectively (for graphs see Supplementary data) were collected on an image plate separately and were found to be almost identical except for the notable changes in the spacing values. The diffractograms of the SmA and SmX phases consisted of a diffuse peak in the wide angle region with d (spacing)-value of 5 Å and 5.2 Å, respectively, which is a characteristic of liquid-like correlations within the smectic planes. Besides, two sharp reflections were observed in the low angle regions for both the phases with the spacing being 34.1 Å and 19.9 Å for the SmA phase and 42.2 Å and 23.6 Å for the SmX phase confirming a layer structure for both the mesophases; the reflections at 19.9 Å and 23.6 Å are the second harmonic and are generally seen in dimeric systems.[23c,d] As can be seen, the layer periodicity in the SmA phase is less than the length (L) of the dimer **TDV-4** (L=43 Å) in its all-trans conformation (measured using Chem3D software); this suggests an intercalated (partially-bilayered) arrangement of the molecules where the mesogenic segments, spacers, and terminal tails are mixed, as schematically shown in Figure 4a. On the other hand, the small angle reflection corresponding to periodicity of 42.2 Å is nearly equal to the length of the molecule, with a d/L ratio of 0.98, indicating the monolayer molecular packing in the SmX phase (Fig. 4b) wherein the mesogenic segments, spacers, and tails form three different regions.

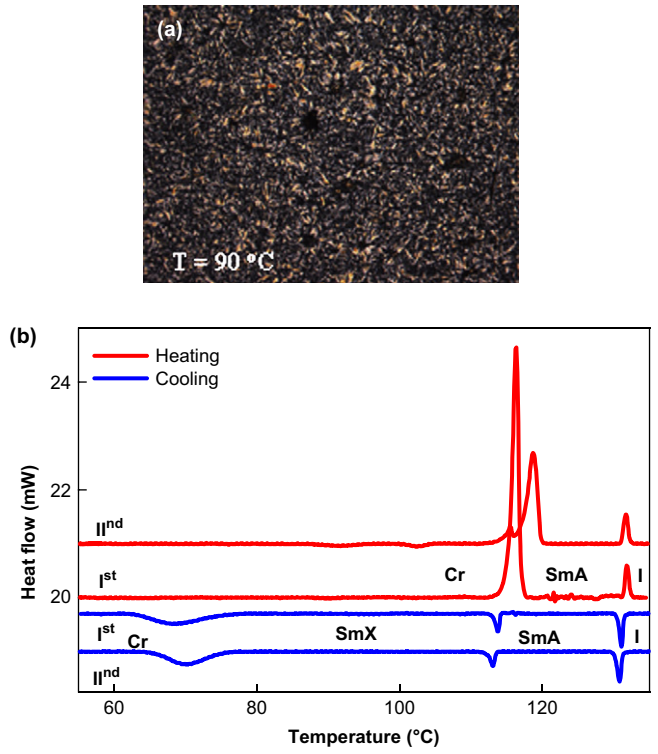

Figure 3. (a) Texture microphotograph of the SmX phase emanated from the pseudoisotropic pattern (homeotropic region) of the preceding SmA phase of compound **TDV-4**. (b) DSC traces obtained during the two successive heating and cooling cycles for the dimer **TDV-4**; notice an exothermic peak due to SmA–SmX phase transition.

It can be seen in Table 1 that all even-members viz., **TDL-3**, **TDL-5**, and **TDL-7** of the **TDL-*n*** series, where the terminal tail is derived from L-leucine, exhibit an enantiotropic dimesomorphic sequence involving a transition from N* phase to SmA phase; Figure 5a shows a texture microphotograph where this phase transition obtained for the dimer **TDL-3** can be seen. Whereas, the dimer **TDL-4** comprising an odd-parity spacer exhibits a monotropic chiral nematic phase. The occurrence of both the mesophases, needless to say, was confirmed by textural observation as described before. All the four compounds of **TDI-*n*** series, which possess a chiral α-chloroalkanoyl tail derived from L-isoleucine, exhibit enantiotropic N*, and SmA phases in addition to a transient TGB phase; this trimesomorphic sequence was established by optical textural observation. On cooling isotropic phase of any one of these four dimers placed between a pair of clean glass sides and observed under POM, a focal-conic texture of the N* phase appears that on shearing transforms to an oily streaks texture. On lowering the temperature from planar texture of the N* phase, the transition to a transient TGB phase occurs with a blurred gray planar texture that rapidly transforms into a focal-conic texture typical of the SmA phase. If the sample is cooled from the natural focal-conic (unsheared) texture of the N* phase, the transition to the SmA was clearly visible where focal-conic as well as pseudoisotropic textures persisted; however, the latter pattern existed predominately, which upon heating (0.1 to 0.5 °C/min) slowly gave a striking filament texture of the TGB phase,[31] see Figure 5b. It may be note here that the TGB phase may have either SmA or smectic C (SmC) slabs.[2]

The important results obtained by analyzing the thermal behavior of these 12 new nonsymmetric dimers are the following. Seemingly, the thermal behavior of dimers belonging to **TDV-*n***, **TDL-*n***, and **TDI-*n*** series, as surmised in parts (a–c) of Figure 6, respectively, shows some dependence on the length and parity of the spacer; the influence of the parity of the spacer on the clearing temperature is especially remarkable. For instance, the dimers **TDV-4**, **TDL-4**, and **TDI-4** comprising an 5-oxypentanoyl (odd-parity; C_5) spacer show lower clearing temperatures; as is well known, such a behavior can be explained in terms of the overall molecular shape of the dimer governed by the geometry and flexibility of the spacer it possesses. The entropy changes associated with isotropic liquid-chiral nematic phase also exhibits odd–even effect for the **TDI-*n*** (see Supplementary data) and **TDL-*n*** (see, Fig. 6d). The space-filling models of energy-minimized molecular structures, deduced from MM2 computations of CS Chem Draw 3D (version 5) program, of dimers **TDV-3** and **TDV-4** are shown in Figure 7a and b, respectively, as representative cases. Apparently, the tolane and cholesterol segments in dimer **TDV-4** are inclined giving a bent molecular shape to the molecule, and thus, the shape anisotropy is reduced accounting for the lower clearing temperatures. It is also perceptible that on increasing the length of the even-parity spacers, except in a few cases, the clearing temperature decreases

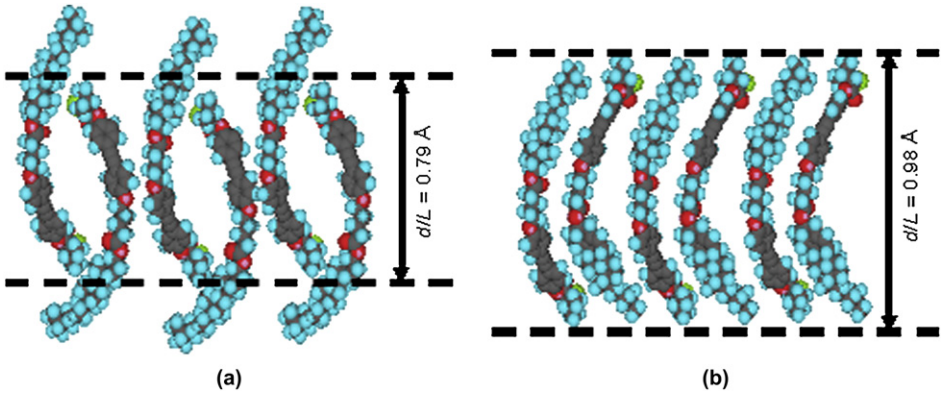

Figure 4. Schematic representation of molecular organizations in an intercalated SmA phase (a) and a fluid monolayer SmX phase (b) formed by the dimer **TDV-4**.

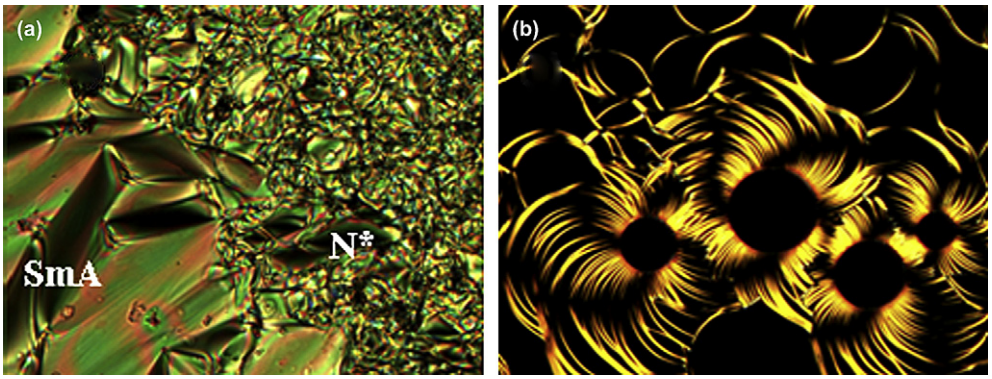

Figure 5. (a) Microphotograph showing characteristic focal-conic texture (left portion) of the SmA phase as seen growing from the N* phase (right portion) of dimer **TDL-3**. (b) Filamentary texture photomicrograph of the TGB phase obtained during the transition from a homeotropically aligned SmA phase to N* phase for the dimer **TDI-3**.

that can be obviously attributed to the higher degree of conformational freedom of the molecules.

Furthermore, the nature of α-chloroalkanoyl tail seems to influence the phase behavior moderately; for example, the compounds of **TDI-*n*** series possessing a terminal derived L-isoleucine, unlike the dimers belonging to **TDV-*n*** and **TDL-*n*** series, exhibit a frustrated phase. Most importantly, contrary to general expectation, none of the dimers synthesized exhibit the SmC* phase; this can be perhaps attributed to the presence of short terminal tail length as well as the bulkiness/non-linearity of the cholesterol, which disfavor the required staggering of the cores.[32]

It is well established that the chiral nematic phase exhibits circular dichroism (CD) where the incident light is resolved into its two circularly polarized components, left and right, at a given wavelength.[1a,33] At this wavelength, depending upon the natural helical sense of the phase, circularly polarized light of a particular handedness is completely reflected while its counterpart is transmitted. Thus, the handedness (screw sense) of the helical array of the phase can be ascertained. Recently, we have reported the first elaborative study on the chiroptical property of the N* phase formed by nonsymmetric chiral dimers; an odd–even effect was evidenced for the selective reflection wavelengths.[34a] Importantly, our study indicated that the N* pitch is right handed for all the studied dimers, which is in agreement with the fact that most steroidal esters are right handed; with a view to obtain a similar information formally, CD measurement was carried out in the neat N* phase of dimer **TDL-4**. The dimer sandwiched between two quartz plates was heated to isotropic phase and cooled slowly with repeated mechanical shearing to attain Grandjean (planar) texture so that the helix of the phase becomes normal to the quartz plates and the structure reflects the incident light. Figure 8 shows temperature dependence of the CD spectra recorded in the N* phase during the cooling cycle. In the CD spectra obtained at temperatures 133 °C, 130 °C, 125 °C, 120 °C, and 115 °C strong positive peaks at λ=364 cm^{-1} (CD=405 mdeg), 373 cm^{-1} (CD=364 mdeg), 377 cm^{-1} (CD=323 mdeg), 379 cm^{-1} (CD=301 mdeg), and 382 cm^{-1} (CD=281 mdeg), respectively, were seen.

Thus, the occurrence of positive pitch band indicates right-handed screw sense of the chiral nematic structure, which is in accordance with our earlier observation that the dimers possessing cholesteryl ester entity are right handed.[34]

As is well known, a large number of drugs and medicinal agents are derived from natural substances; they have advantages over synthetic compounds owing to their diverse structural features with remarkable biological activity.[35] Besides, they offer several ways of amending their molecular structure such that the molecular material features such as self-organizing ability, fluidity, molecular recognition can be imbued. For example, as discussed above, cholesterol and its derivatives are not only familiar in the area of supramolecular chemistry,[14] but also in health care.[36] Likewise, the amino acid derivatives are widely recognized for their biological significance.[37] As discussed earlier, tolane core has now been considered as an important building block to generate biologically active compounds. Given the fact that such promising components are incorporated in nonsymmetric dimers of the present investigation, we were motivated to examine their biological property. As a first step in this direction, we intended to evaluate antimicrobial activity of a representative compound. Thus, an indiscriminately selected dimer **TDI-5** was subjected for antibacterial and antifungal screening by disc diffusion technique (DDT); the results obtained are tabulated in Table 2. DDT was carried out using molten Muller Hinton agar media. The inoculum size was standardized under aseptic condition such that each mL contains 108 cells. The inoculum was uniformly inoculated using sterile cotton swab. Dimer **TDI-5** (200 μL, 1 mg/mL) was placed at regular intervals over inoculated medium using Whatmann No. 2 filter paper disc of 6 mm in diameter. The plates were then incubated at 37 °C for 24 h. The zone of inhibition was read using zone reader, Ciprofloxcin and Clotrimazole of 10 μg/disc potency was used as standard discs for bacteria and fungi, respectively, as shown in zone plate photographs (see Supplementary data).

Apparently, the dimer shows some marked activity against *Candida albicans*; for other microbes it showed little activity. However, resistance (inhibition) was observed against *Staphylococcus albus* and *Staphylococcus faecalis*. This preliminary

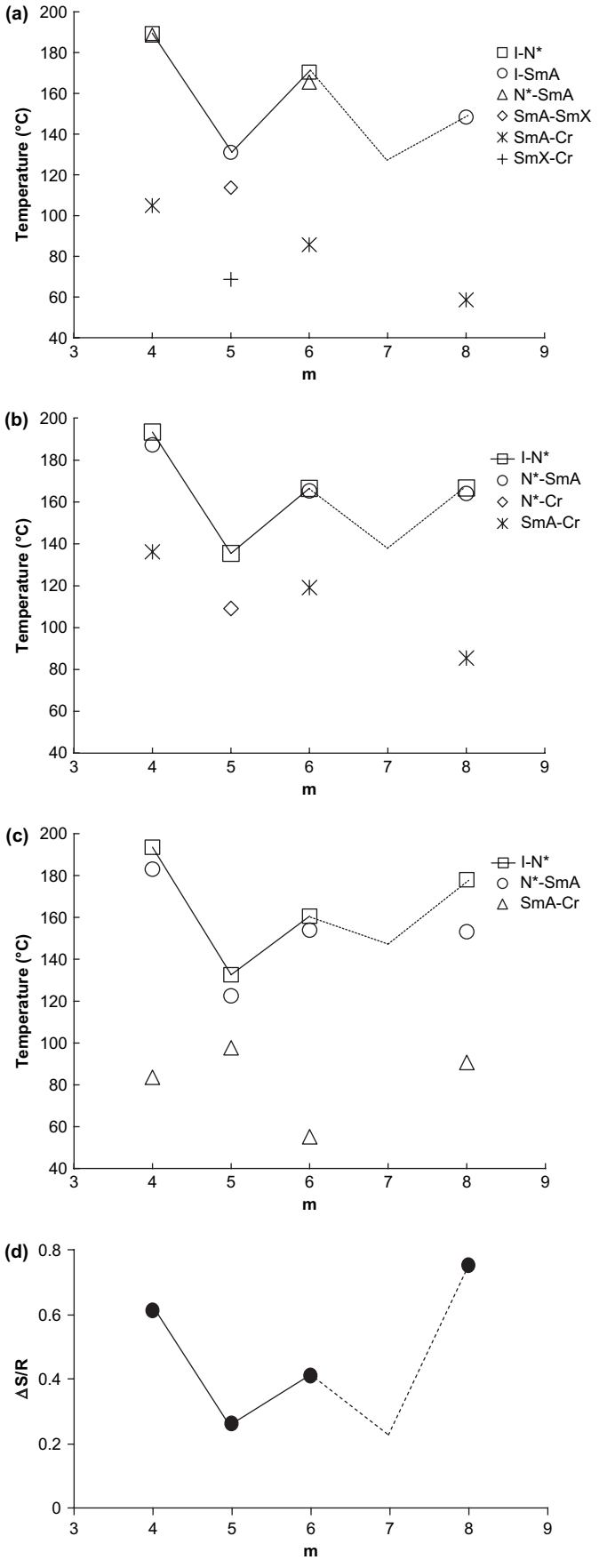

Figure 6. The influence of the number of carbon atoms m (n+1) in the ω-oxyalkanoyl spacer on the transition temperatures for **TDV-*n*** (a), **TDL-*n*** (b), and **TDI-*n*** (c). Note that in **TDI-*n*** series phase diagram (c), the TGB phase has not been included owing to its transient nature (for details see Table 1). Also shown is the dependence of isotropic liquid-chiral nematic phase transition entropy on the number of carbon atoms (m) in the ω-oxyalkanoyl spacer of **TDL-*n*** series (d). In all the plots dashed lines joining points are suggestive of the general trend; it may be noted that experimental data do not cover for n=7.

study indicates that nonsymmetric dimers having pro-bioactive components could be of some pharmacological interest; indeed, a systematic study involving design and synthesis of such dimers with variations in their molecular fragment/s is essential to prove their real credibility.

3.2. Summary

Twelve new optically active nonsymmetric dimers have been synthesized and their liquid crystal behavior is investigated. Specifically, in order to study structure–property relationships of cholesterol-based dimers comprising tolane segment, and to evaluate the effect of different α-chloroalkanoyl tails on the phase behavior, three different series of dimers have been studied. In each series, the length and parity of the spacer is varied while the chiral α-chloroalkanoyl tail is held constant. The experimental results show that both the spacer parity and the nature of terminal tail influence the thermal behavior. The former affects the clearing temperature significantly; the dimers comprising even-parity spacer show higher values. Whereas, the latter seems to play an important role in deciding the phase sequence; the dimers possessing α-chloro ester group derived from L-valine/L-leucine stabilize chiral nematic and/or smectic phase/s, while the systems with terminal group resulting from L-isoleucine show twist grain boundary phase additionally. For an odd-parity dimer with an α-chloro ester group derived from L-valine, the occurrence of a transition from intercalated smectic A phase to an unknown smectic phase with monolayer molecular packing has been established by XRD study. To explore the biological activity, one of the randomly selected dimer has been screened for antibacterial and antifungal activities by disc diffusion method; the dimer seems to be active against some microbes.

4. Experimental

4.1. General information

The requisite precursors were purchased either from Aldrich or Lancaster Company and used as received. Solvents were purified and dried by literature methods prior to the use. Crude compounds were purified by column chromatographic technique using either silica gel (400 mesh) or neutral aluminum oxide as a stationary phase. Thin layer chromatography (TLC) was performed on aluminum sheets pre-coated with silica gel (Merck, Kieselgel 60, F_{254}). Absorption spectra were recorded on a Perkin–Elmer Lambda 20 UV–Vis

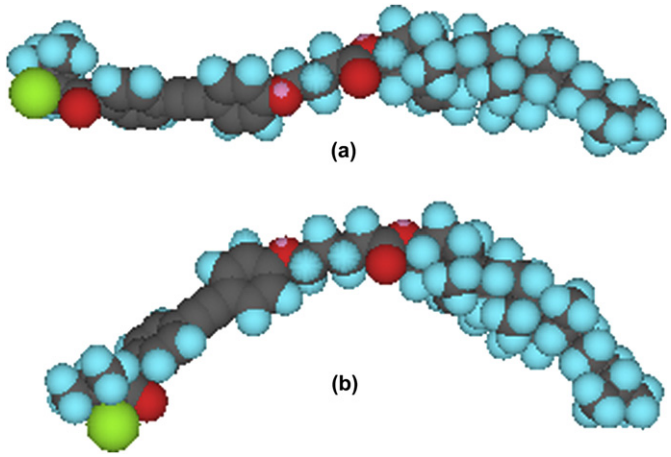

Figure 7. Space-filling models of energy-minimized molecular structures of dimers **TDV-3** (a) and **TDV-4** (b); notice that in the later case the tolane and cholesterol entities are leaning.

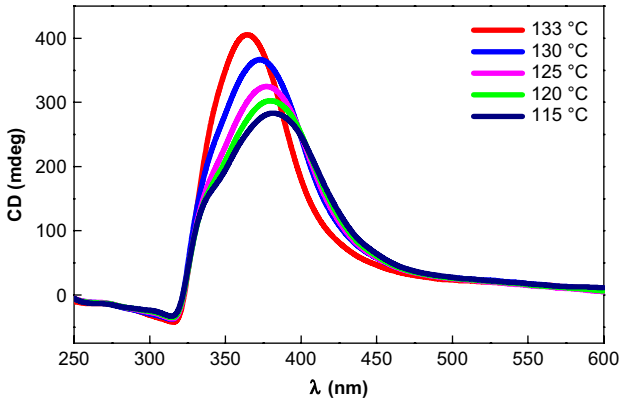

Figure 8. Temperature dependence of the CD spectra of the N* phase recorded in the cooling cycle for dimer **TDL-4**.

Table 2
Results of antimicrobial (antibacterial and antifungal) activity measured by DDT

Organism	Diameter of the inhibition zone (in mm)	
	TDI-5	Standard
Staphylococcus aureus	15	30
Staphylococcus albus	R[a]	35
Staphylococcus faecalis	R[a]	40
Escherichia coli	14	24
Pseudomonas aeruginosa	20	40
Klebsiella aerogenes	15	35
Proteus vulgaris	13	25
Candida albicans	20	26

[a] Resistance.

spectrometer. IR spectra were recorded using Perkin–Elmer Spectrum 1000 FT-IR spectrometer. ^{1}H NMR spectra were recorded using either a Bruker AMX-400 (400 MHz) or a Bruker Aveance series DPX-200 (200 MHz) spectrometer and the chemical shifts are reported in parts per million (ppm) relative to tetramethylsilane (TMS) as an internal standard. Mass spectra were recorded on a Jeol-JMS-600H spectrometer in FAB$^+$ mode using 3-nitrobenzyl alcohol as a liquid matrix. Elemental analyses were done using Eurovector model EA 3000 CHNS analyzer. The specific rotation of the target molecules was measured using a JASCO DIP-370 digital polarimeter. CD measurements were carried out using Jasco J-810 spectropolarimeter. The identification of the mesophases and the transition temperatures of the compounds were initially determined using a polarizing microscope (Leitz DMRXP) in conjunction with a programmable hot stage (Mettler FP90). The phase transition temperatures and associated enthalpies were determined from thermograms recorded at a scanning rate of 5 °C/min on a differential scanning calorimeter (DSC; Perkin–Elmer DSC-7 with the PC system operating on *Pyris* software) apriorically calibrated using pure indium as a standard. The energy-minimized space-filling molecular structures of dimers were obtained using MM2 computations of the CS *ChemDraw3D* (version 5) program. The X-ray measurements were performed using Cu Kα radiations (λ=1.5418 Å) from a fine focus sealed-tube generator (Enraf Nonius FR590), in conjunction with double mirror focusing optics. The detector employed was an image plate detector (MAC Science, Japan; Model DIP 1030).

*4.2. General procedure for the synthesis of **TDV-n**, **TDL-n**, and **TDI-n** series of dimers*

The α-chloro acid (**1a–c**) (3.3 mmol, 1.0 equiv) was taken in a two-necked round bottomed flask under nitrogen atmosphere to which oxalyl chloride (10 mmol, 3 equiv) was added. The reaction mixture was stirred at room temperature for 4 h. The excess of oxalyl chloride was distilled off under reduced pressure. The acid chloride obtained was thoroughly dried under vacuo to which a mixture of cholesteryl ω-[(4-hydroxyphenylethynyl)-4-phenoxy]alkanoates (**8a–d**) (0.15 mmol, 1.0 equiv) and pyridine (0.5 mL) in dry THF (10 mL) was added drop wise at 0 °C. The reaction mixture was slowly allowed to attain room temperature and continued to stir for 12 h. The reaction mixture was filtered on Celite bed; after evaporating the solvent from the filtrate, a colorless mass was obtained that was dissolved in CH_2Cl_2. The organic layer was thoroughly washed with 3 N $HCl_{(aq)}$ (2×10 ml), 5% solution of $NaOH_{(aq)}$ (2×10 ml), water (2×10 ml), brine, and dried over anhydrous Na_2SO_4. The crude mass obtained upon evaporation of the solvent was purified by column chromatography on silica gel (100–200 mesh). Elution with a mixture of 5% of EtOAc–hexanes afforded the product. It was further purified by repeated recrystallizations from a mixture of EtOH–CH_2Cl_2 (9:1) to get a pure white solid.

*4.2.1. Cholesteryl 4-[(4-(2-chloro-3-methylbutanoyloxy)-phenylethynyl)-4-phenoxy]butanoate (**TDV-3**)*

R_f=0.40 in 10% EtOAc–hexane; yield: 75%; IR (KBr pellet) ν_{max} in cm^{-1}: 2951, 2219, 1772, 1718, 1607, 1247, 1197, 1163, 770; UV–vis: λ_{max}=311.6 nm, ε=2.59×10^4 L mol^{-1} cm^{-1}; $[\alpha]_D^{22}$ −13.2 (*c* 1.0, $CHCl_3$); ^{1}H NMR (400 MHz, $CDCl_3$): δ 7.54 (d, *J*=9.1 Hz, 2H, Ar), 7.45 (d, *J*=8.8 Hz, 2H, Ar), 7.11 (d, *J*=8.2 Hz, 2H, Ar), 6.86 (d, *J*=8.8 Hz, 2H, Ar), 5.37 (br d, *J*=3.7 Hz, 1H, 1×olefinic),

4.64 (m, 1H, 1×CHOCO), 4.33 (d, J=6.6 Hz, 1H, CHCl), 4.04 (t, J=6.1 Hz, 2H, 1×OCH_2), 2.49–1.05 (m, 33H, 7×CH, 2×allylic methylene, 11×CH_2), 1.04 (s, 3H, 1×CH_3), 1.01 (s, 3H, 1×CH_3), 0.98 (s, 3H, 1×CH_3), 0.92 (d, J=6.5 Hz, 3H, 1×CH_3), 0.87 (d, J=1.6 Hz, 3H, 1×CH_3), 0.85 (d, J=1.6 Hz, 3H, 1×CH_3), 0.67 (s, 3H, 1×CH_3); ^{13}C NMR (100 MHz, $CDCl_3$): 172.49, 168.24, 159.05, 149.91, 139.63, 133.07, 132.65, 122.69, 121.89, 121.20, 115.16, 114.58, 89.79, 86.08, 74.13, 66.89, 63.85, 56.71, 56.17, 55.65, 50.05, 43.39, 42.33, 39.75, 39.52, 38.15, 26.98, 36.60, 36.19, 35.78, 35.78, 31.89, 31.08, 28.99, 28.22, 28.01, 27.82, 25.31, 24.65, 24.28, 23.83, 22.80, 22.55, 21.48, 21.04, 19.30, 18.72, 18.20, 11.71, 10.69; MS (FAB+): *m/z* calcd for $C_{50}H_{67}ClO_5$: 782.47. Found: 782.52; Anal. Calcd for $C_{50}H_{67}ClO_5$: C, 76.65; H, 8.62. Found: C, 76.88; H, 8.78.

4.2.2. Cholesteryl 5-[(4-(2-chloro-3-methylbutanoyloxy)-phenylethynyl)-4-phenoxy]pentanoate (**TDV-4**)

R_f=0.40 in 10% EtOAc–hexane; yield: 71%; IR (KBr pellet) ν_{max} in cm^{-1}: 2938, 2220, 1771, 1733, 1607, 1250, 1197, 1174, 660; UV–vis: λ_{max}=312.1 nm, ε=3.22×10^4 L mol^{-1} cm^{-1}; $[\alpha]_D^{22}$ −10.1 (*c* 1.0, $CHCl_3$); ^{1}H NMR (400 MHz, $CDCl_3$): δ 7.53 (d, J=8.6 Hz, 2H, Ar), 7.45 (d, J=8.8 Hz, 2H, Ar), 7.10 (d, J=8.6 Hz, 2H, Ar), 6.8 (d, J=6.8 Hz, 2H, Ar), 5.37 (br d, J=3.8 Hz, 1H, 1×olefinic), 4.3 (d, J=6.6 Hz, 1H, CHCl), 4.6 (m, 1H, 1×CHOCO), 3.99 (t, J=3.8 Hz, 2H, 1×OCH_2), 2.45–1.05 (m, 35H, 7×CH, 2×allylic methylene, 12×CH_2), 1.03 (s, 3H, 1×CH_3), 1.01 (s, 3H, 1×CH_3), 0.98 (s, 3H, 1×CH_3), 0.91 (d, J=6.5 Hz, 3H, 1×CH_3), 0.87 (d, J=1.6 Hz, 3H, 1×CH_3), 0.85 (d, J=1.6 Hz, 3H, 1×CH_3), 0.67 (s, 3H, 1×CH_3); ^{13}C NMR (100 MHz, $CDCl_3$): 173.21, 168.30, 159.33, 149.85, 139.71, 133.05, 132.64, 122.61, 121.95, 121.25, 114.86, 114.57, 89.89, 86.98, 73.75, 67.99, 63.90, 56.70, 56.16, 50.04, 43.40, 42.32, 39.74, 39.52, 39.14, 38.17, 36.99, 36.60, 36.19, 35.79, 34.64, 32.79, 31.89, 28.98, 28.21, 28.01, 27.83, 25.83, 24.94, 24.28, 23.83, 22.80, 22.54, 21.03, 19.30, 18.72, 18.21, 11.68, 10.80; MS (FAB+): *m/z* calcd for $C_{51}H_{69}ClO_5$: 796.48. Found: 796.46; Anal. Calcd for $C_{51}H_{69}ClO_5$: C, 76.80; H, 8.72. Found: C, 77.07; H, 8.52.

4.2.3. Cholesteryl 6-[(4-(2-chloro-3-methylbutanoyloxy)-phenylethynyl)-4-phenoxy]hexanoate (**TDV-5**)

R_f=0.40 in 10% EtOAc–hexane; yield: 70%; IR (KBr pellet) ν_{max} in cm^{-1}: 2935, 2215, 1769, 1728, 1606, 1249, 1198, 1165, 649; UV–vis: λ_{max}=312 nm, ε=3.01×10^4 L mol^{-1} cm^{-1}; $[\alpha]_D^{22}$ −9.1 (*c* 1.0, $CHCl_3$); ^{1}H NMR (400 MHz, $CDCl_3$): δ 7.53 (d, J=8.6 Hz, 2H, Ar), 7.45 (d, J=8.7 Hz, 2H, Ar), 6.86 (d, J=8.7 Hz, 2H, Ar), 7.10 (d, J=8.6 Hz, 2H, Ar), 5.37 (br d, J=3.7 Hz, 1H, 1×olefinic), 4.62 (m, 1H, 1×CHOCO), 4.33 (d, J=6.6 Hz, 1H, CHCl), 3.97 (t, J=6.4 Hz, 2H, 1×OCH_2), 2.45–1.05 (m, 37H, 7×CH, 2×allylic methylene, 13×CH_2), 1.03 (s, 3H, 1×CH_3), 1.01 (s, 3H, 1×CH_3), 0.98 (s, 3H, 1×CH_3), 0.93 (d, J=8.2 Hz, 3H, 1×CH_3), 0.87 (d, J=1.6 Hz, 3H, 1×CH_3), 0.85 (d, J=1.6 Hz, 3H, 1×CH_3), 0.67 (s, 3H, 1×CH_3); ^{13}C NMR (100 MHz, $CDCl_3$): 173.00, 168.26, 159.23, 149.86, 139.66, 133.05, 132.63, 122.63, 121.91, 121.20, 114.92, 114.54, 89.85, 87.00, 73.83, 67.71, 63.70, 56.69, 56.14, 50.03, 43.37, 42.31, 39.73, 39.51, 39.10, 38.16, 36.98, 36.59, 36.18, 35.78, 34.55, 32.70, 31.89, 28.86, 28.21, 28.01, 27.82, 25.57, 24.76, 24.27, 23.82, 22.80, 22.56, 21.47, 19.31, 18.71, 18.20, 11.70, 10.81; MS (FAB+): *m/z* calcd for $C_{52}H_{71}ClO_5$: 810.50. Found: 810.57; Anal. Calcd for $C_{52}H_{71}ClO_5$: C, 76.96; H, 8.82. Found: C, 77.03; H, 8.80.

4.2.4. Cholesteryl 8-[(4-(2-chloro-3-methylbutanoyloxy)-phenylethynyl)-4-phenoxy]octanoate (**TDV-7**)

R_f=0.40 in 10% EtOAc–hexane; yield: 70%; IR (KBr pellet) ν_{max} in cm^{-1}: 2938, 2219, 1770, 1728, 1606, 1249, 1198, 1163, 749; UV–vis: λ_{max}=312.1 nm, ε=3.01×10^4 L mol^{-1} cm^{-1}; $[\alpha]_D^{22}$ −9.7 (*c* 1.0, $CHCl_3$); ^{1}H NMR (400 MHz, $CDCl_3$): δ 7.53 (d, J=8.6 Hz, 2H, Ar), 7.45 (d, J=8.7 Hz, 2H, Ar), 7.10 (d, J=8.6 Hz, 2H, Ar), 6.86 (d, J=8.7 Hz, 2H, Ar), 5.37 (br d, J=3.9 Hz, 1H, 1×olefinic), 4.60 (m, 1H, 1×CHOCO), 4.3 (d, J=6.6 Hz, 1H, CHCl), 3.99 (t, J=6.3 Hz, 2H, 1×OCH_2), 2.45–1.05 (m, 41H, 7×CH, 2×allylic methylene, 15×CH_2), 1.03 (s, 3H, 1×CH_3), 1.01 (s, 3H, 1×CH_3), 0.98 (s, 3H, 1×CH_3), 0.92 (d, J=6.4 Hz, 3H, 1×CH_3), 0.87 (d, J=1.6 Hz, 3H, 1×CH_3), 0.85 (d, J=1.6, 3H, 1×CH_3), 0.67 (s, 3H, 1×CH_3); ^{13}C NMR (100 MHz, $CDCl_3$): 173.01, 167.45, 159.60, 149.23, 139.71, 133.20, 132.65, 127.81, 127.40, 122.69, 121.85, 121.26, 116.00, 109.39, 68.52, 62.80, 58.65, 51.50, 50.98, 44.87, 34.55, 32.96, 31.80, 30.98, 30.55, 29.42, 25.59, 23.73, 23.10, 22.61, 20.59, 19.71, 19.05, 17.30, 15.82, 14.36, 14.05, 12.97, 10.91; MS (FAB+): *m/z* calcd for $C_{54}H_{75}ClO_5$: 838.53. Found: 838.71; Anal. Calcd for $C_{54}H_{75}ClO_5$: C, 77.25; H, 9.0. Found: C, 77.60; H, 8.87.

4.2.5. Cholesteryl 4-[(4-(2-chloro-4-methylpentanoyloxy)-phenylethynyl)-4-phenoxy]butanoate (**TDL-3**)

R_f=0.74 in 10% EtOAc–hexanes; yield: 70%; IR (KBr pellet): ν_{max} in cm^{-1}: 2950, 2218, 1765, 1724, 1606, 1247, 1196, 1164, 768; UV–vis: λ_{max}=311.7 nm, ε=2.53×10^4 L mol^{-1} cm^{-1}; $[\alpha]_D^{22}$ −11.7 (*c* 1.0, $CHCl_3$); ^{1}H NMR (400 MHz, $CDCl_3$): δ 7.53 (d, J=8.5 Hz, 2H, Ar), 7.45 (d, J=8.6 Hz, 2H, Ar), 7.11 (d, J=8.5 Hz, 2H, Ar), 6.87 (d, J=8.6 Hz, 2H, Ar), 5.38 (br d, J=4.8 Hz, 1H, 1×olefinic), 4.62 (m, 1H, 1×CHOCO), 4.52 (t, J=7.4 Hz, 1H, CHCl), 4.02 (t, J=6.1, 2H, 1×OCH_2), 2.50–1.06 (m, 35H, 7×CH, 2×allylic methylene, 12×CH_2), 1.04 (s, 3H, 1×CH_3), 1.01 (s, 3H, 1×CH_3), 0.98 (s, 3H, 1×CH_3), 0.92 (d, J=6.4 Hz, 3H, 1×CH_3), 0.86 (d, J=1.4 Hz, 3H, 1×CH_3), 0.85 (d, J=1.4 Hz, 3H, 1×CH_3), 0.67 (s, 3H, 1×CH_3); ^{13}C NMR (100 MHz, $CDCl_3$): 172.49, 167.65, 159.06, 149.88, 139.63, 133.07, 132.65, 122.69, 121.89, 121.25, 115.16, 114.58, 89.78, 87.08, 74.12, 66.88, 63.88, 56.70, 56.16, 50.05, 42.32, 39.74, 39.52, 39.03, 38.15, 36.99, 36.60, 36.19, 35.78, 34.45, 32.78, 31.89, 28.20, 27.99, 27.81, 24.64, 24.27, 23.83, 22.78, 22.54, 21.03, 19.61, 19.29, 18.72, 18.21, 11.84, 10.80; MS (FAB+): *m/z* calcd for $C_{51}H_{69}ClO_5$: 796.48. Found: 796.5; Anal. Calcd for $C_{51}H_{69}ClO_5$: C, 76.80; H, 8.72. Found: C, 77.01; H, 8.45.

*4.2.6. Cholesteryl 5-[(4-(2-chloro-4-methylpentanoyloxy)-phenylethynyl)-4-phenoxy]pentanoate (**TDL-4**)*

R_f=0.74 in 10% EtOAc–hexanes; yield: 71%; IR (KBr pellet) ν_{max} in cm^{-1}: 2955, 2216, 1752, 1727, 1606, 1246, 1190, 1167, 772; UV–vis: λ_{max}=312 nm, ε=3.18×10^4 L mol^{-1} cm^{-1}; $[\alpha]_D^{22}$ −8.7 (*c* 1.0, $CHCl_3$); ^{1}H NMR (400 MHz, $CDCl_3$): δ 7.53 (d, *J*=8.6 Hz, 2H, Ar), 7.45 (d, *J*=8.9 Hz, 2H, Ar), 7.11 (d, *J*=8.7 Hz, 2H, Ar), 6.86 (d, *J*=8.8 Hz, 2H, Ar), 5.37 (br d, *J*=3.9 Hz, 1H, 1×olefinic), 4.6 (t, *J*=7.4 Hz, 1H, CHCl), 4.2 (m, 1H, 1×CHOCO), 3.99 (t, *J*=5.2 Hz, 2H, 1×OCH_2), 2.38–1.05 (m, 37H, 7×CH, 2×allylic methylene, 13×CH_2), 1.04 (s, 3H, 1×CH_3), 1.01 (s, 3H, 1×CH_3), 0.98 (s, 3H, 1×CH_3), 0.92 (d, *J*=6.4 Hz, 3H, 1×CH_3), 0.86 (d, *J*=1.6 Hz, 3H, 1×CH_3), 0.85 (d, *J*=1.6 Hz, 3H, 1×CH_3), 0.67 (s, 3H, 1×CH_3); ^{13}C NMR (100 MHz, $CDCl_3$): 172.82, 168.84, 159.13, 149.80, 139.65, 133.06, 132.64, 122.66, 121.92, 121.26, 115.47, 115.03, 114.57, 89.90, 87.04, 73.96, 67.48, 63.89, 56.70, 56.16, 50.05, 42.32, 39.74, 39.52, 39.16, 38.16, 36.99, 36.60, 36.19, 35.78, 34.27, 32.79, 31.89, 28.57, 28.19, 28.01, 27.82, 25.87, 24.93, 27.28, 23.84, 22.79, 22.55, 21.69, 21.04, 19.62, 19.30, 18.71, 18.20, 11.66, 10.75; MS (FAB+): *m/z* calcd for $C_{52}H_{71}ClO_5$: 810.50. Found: 810.45; Anal. Calcd for $C_{52}H_{71}ClO_5$: C, 76.96; H, 8.82. Found: C, 77.02; H, 8.79.

*4.2.7. Cholesteryl 6-[(4-(2-chloro-4-methylpentanoyloxy)-phenylethynyl)-4-phenoxy]hexanoate (**TDL-5**)*

R_f=0.74 in 10% EtOAc–hexanes; yield: 72%; IR (KBr pellet) ν_{max} in cm^{-1}: 2937, 2217, 1764, 1731, 1606, 1247, 1199, 1166, 772; UV–vis: λ_{max}=312 nm, ε=4.15×10^4 L mol^{-1} cm^{-1}; $[\alpha]_D^{22}$ −13.7 (*c* 1.0, $CHCl_3$); ^{1}H NMR (400 MHz, $CDCl_3$): δ 7.53 (d, *J*=8.6 Hz, 2H, Ar), 7.45 (d, *J*=8.7 Hz, 2H, Ar), 6.86 (d, *J*=8.7 Hz, 2H, Ar), 7.09 (d, *J*=8.6 Hz, 2H, Ar), 5.37 (br d, *J*=4.0 Hz, 1H, 1×olefinic), 4.62 (m, 1H, 1×CHOCO), 4.53 (t, *J*=7.3 Hz, 1H, CHCl), 3.96 (t, *J*=6.4 Hz, 2H, 1×OCH_2), 2.31–1.05 (m, 39H, 7×CH, 2×allylic methylene, 14×CH_2) 1.04 (s, 3H, 1×CH_3), 1.01 (s, 3H, 1×CH_3), 0.98 (s, 3H, 1×CH_3), 0.91 (d, *J*=6.4 Hz, 3H, 1×CH_3), 0.87 (d, *J*=1.5 Hz, 3H, 1×CH_3), 0.85 (d, *J*=1.5 Hz, 3H, 1×CH_3), 0.67 (s, 3H, 1×CH_3); ^{13}C NMR (100 MHz, $CDCl_3$): 172.99, 167.66, 159.25, 149.85, 139.68, 133.06, 132.64, 122.64, 121.93, 121.25, 114.93, 114.56, 89.86, 87.01, 73.84, 67.72, 63.89, 56.70, 56.16, 50.04, 42.31, 39.74, 39.52, 39.04, 38.16, 36.99, 36.60, 36.18, 35.78, 34.55, 32.78, 31.88, 28.85, 28.21, 28.00, 27.82, 25.57, 24.76, 24.27, 23.83, 22.79, 22.54, 21.0., 19.62, 19.30, 18.71, 18.20, 11.80, 10.75; MS (FAB+): *m/z* calcd for $C_{53}H_{73}ClO_5$: 824.15. Found: 824.68; Anal. Calcd for $C_{53}H_{73}ClO_5$: C, 77.10; H, 8.91. Found: C, 77.25; H, 8.45.

*4.2.8. Cholesteryl 8-[(4-(2-chloro-4-methylpentanoyloxy)-phenylethynyl)-4-phenoxy]octanoate (**TDL-7**)*

R_f=0.74 in 10% EtOAc–hexane; yield: 69%; IR (KBr pellet) ν_{max} in cm^{-1}: 2949, 2217, 1762, 1732, 1606, 1248, 1199, 1163, 773; UV–vis: λ_{max}=312.1 nm, ε=2.37×10^4 L mol^{-1} cm^{-1}; $[\alpha]_D^{22}$ −10.5 (*c* 1.0, $CHCl_3$); ^{1}H NMR (400 MHz, $CDCl_3$): δ 7.53 (d, *J*=8.68 Hz, 2H, Ar), 7.45 (d, *J*=8.76 Hz, 2H, Ar), 7.11 (d, *J*=8.7 Hz, 2H, Ar), 6.86 (d, *J*=8.8 Hz, 2H, Ar), 5.37 (br d, *J*=3.8 Hz, 1H, 1×olefinic), 4.60 (m, 1H, 1×CHOCO), 4.53 (t, *J*=7.3 Hz, 1H, CHCl), 3.97 (t, *J*=6.3 Hz, 2H, 1×OCH_2), 2.33–1.05 (m, 43H, 7×CH, 2×allylic methylene, 16×CH_2), 1.03 (s, 3H, 1×CH_3), 1.01 (s, 3H, 1×CH_3), 0.98 (s, 3H, 1×CH_3), 0.91 (d, *J*=6.5 Hz, 3H, 1×CH_3), 0.87 (d, *J*=1.6 Hz, 3H, 1×CH_3), 0.85 (d, *J*=1.6 Hz, 3H, 1×CH_3), 0.67 (s, 3H, 1×CH_3); ^{13}C NMR (100 MHz, $CDCl_3$): 172.99, 167.66, 159.25, 149.85, 139.68, 133.06, 132.64, 122.64, 121.93, 121.25, 114.93, 114.56, 89.86, 87.01, 73.84, 67.72, 63.89, 56.70, 56.16, 50.04, 42.31, 39.74, 39.52, 39.07, 38.16, 36.99, 36.60, 36.18, 35.78, 34.55, 32.78, 31.88, 28.85, 28.21, 28.00, 27.82, 25.57, 24.76, 24.27, 23.82, 22.79, 22.54, 21.03, 19.62, 19.30, 18.71, 18.19, 11.83, 10.76; MS (FAB+): *m/z* calcd for $C_{55}H_{77}ClO_5$: 852.55. Found: 853; Anal. Calcd for $C_{55}H_{77}ClO_5$: C, 77.38; H, 9.09. Found: C, 77.24; H, 8.82.

*4.2.9. Cholesteryl 4-[(4-(2-chloro-3-methylpentanoyloxy)-phenylethynyl)-4-phenoxy]butanoate (**TDI-3**)*

R_f=0.42 in 10% EtOAc–hexanes; yield: 65%; IR (KBr pellet) ν_{max} in cm^{-1}: 2946, 2219, 1763, 1727, 1607, 1246, 1198, 1164, 770; UV–vis: λ_{max}=312 nm, ε=2.75×10^4 L mol^{-1} cm^{-1}; $[\alpha]_D^{22}$ −8.3 (*c* 1.0, $CHCl_3$); ^{1}H NMR (400 MHz, $CDCl_3$): δ 7.53 (d, *J*=8.6 Hz, 2H, Ar), 7.45 (d, *J*=8.7 Hz, 2H, Ar), 7.11 (d, *J*=8.6 Hz, 2H, Ar), 6.87 (d, *J*=8.7 Hz, 2H, Ar), 5.37 (br d, J=3.7 Hz, 1H, 1×olefinic), 4.64 (m, 1H, 1×CHOCO), 4.37 (d, *J*=7.0 Hz, 1H, CHCl), 4.04 (t, *J*=6.0 Hz, 2H, 1×OCH_2), 2.50–1.05 (m, 35H, 7×CH, 2×allylic methylene, 12×CH_2), 1.02 (s, 3H, 1×CH_3), 1.01 (s, 3H, 1×CH_3), 0.98 (s, 3H, 1×CH_3), 0.92 (d, *J*=8.5 Hz, 3H, 1×CH_3), 0.87 (d, *J*=1.6 Hz, 3H, 1×CH_3), 0.85 (d, *J*=1.6 Hz, 3H, 1×CH_3), 0.67 (s, 3H, 1×CH_3); ^{13}C NMR (100 MHz, $CDCl_3$): 172.77, 167.65, 159.14, 149.65, 139.65, 133.06, 132.63, 122.65, 121.90, 121.25, 115.03, 114.57, 89.83, 87.04, 73.94, 67.48, 62.55, 56.70, 56.16, 50.05, 42.32, 39.74, 39.04, 39.04, 38.16, 36.99, 36.60, 36.19, 35.78, 34.26, 31.89, 31.89, 28.56, 28.21, 28.01, 27.83, 25.15, 24.27, 23.83, 22.79, 22.54, 21.69, 21.04, 19.30, 18.71, 15.96, 11.84, 10.85; MS (FAB+): *m/z* calcd for $C_{51}H_{69}ClO_5$: 796.48. Found: 796.55; Anal. Calcd for $C_{51}H_{69}ClO_5$: C, 76.80; H, 8.72. Found: C, 77.01; H, 8.66.

*4.2.10. Cholesteryl 5-[(4-(2-chloro-3-methylpentanoyloxy)-phenylethynyl)-4-phenoxy]pentanoate (**TDI-4**)*

R_f=0.42 in 10% EtOAc–hexane; yield: 70%; IR (KBr pellet) ν_{max} in cm^{-1}: 2938, 2216, 1770, 1730, 1607, 1250, 1196, 1174, 740; UV–vis: λ_{max}=312.1 nm, ε=2.75×104 L mol^{-1} cm^{-1}; $[\alpha]_D^{22}$ −10.3 (*c* 1.0, $CHCl_3$); ^{1}H NMR (400 MHz, $CDCl_3$): δ 7.53 (d, *J*=8.7 Hz, 2H, Ar), 7.45 (d, *J*=8.8 Hz, 2H, Ar), 7.10 (d, *J*=1.8 Hz, 2H, Ar), 6.8 (d, *J*=8.8 Hz, 2H, Ar), 5.37 (br d, *J*=3.8 Hz, 1H, 1×olefinic), 4.6 (m, 1H, 1×CHOCO), 4.3 (d, *J*=7.0 Hz, 1H, CHCl), 3.99 (t, *J*=5.3 Hz, 2H, 1×OCH_2), 2.38–1.05 (m, 37H, 7×CH, 2×allylic methylene, 13×CH_2), 1.03 (s, 3H, 1×CH_3), 1.01 (s, 3H, 1×CH_3), 0.98 (s, 3H, 1×CH_3), 0.92 (d, *J*=6.48 Hz,

3H, 1×CH_3), 0.87 (d, J=1.6 Hz, 3H, 1×CH_3), 0.85 (d, J=1.6 Hz, 3H, 1×CH_3), 0.67 (s, 3H, 1×CH_3); ^{13}C NMR (100 MHz, $CDCl_3$): 172.78, 167.80, 159.21, 149.20, 139.71, 133.10, 132.67, 122.68, 121.95, 121.28, 115.24, 114.64, 89.80, 87.63, 73.99, 67.56, 62.58, 56.77, 56.24, 50.13, 42.38, 39.81, 39.57, 39.10, 38.21, 37.04, 36.66, 36.24, 35.82, 34.30, 31.94, 30.87, 28.61, 28.24, 28.03, 27.87, 25.21, 24.31, 23.88, 22.80, 22.56, 21.73, 21.09, 19.33, 18.75, 15.98, 11.88, 10.87; MS (FAB+): *m/z* calcd for $C_{52}H_{71}ClO_5$: 810.50. Found: 810.54; Anal. Calcd for $C_{52}H_{71}ClO_5$: C, 76.96; H, 8.82. Found: C, 77.02; H, 8.85.

*4.2.11. Cholesteryl 6-[(4-(2-chloro-3-methylpentanoyloxy)-phenylethynyl)-4-phenoxy]hexanoate (**TDI-5**)*

R_f=0.42 in 10% EtOAc–hexane; yield: 65%; IR (KBr pellet) ν_{max} in cm^{-1}: 2940, 2214, 1767, 1723, 1608, 1249, 1198, 1167, 760; UV–vis: λ_{max}=312.1 nm, ε=3.09×10^4 L mol^{-1} cm^{-1}; $[\alpha]_D^{22}$ −10.7 (*c* 1.0, $CHCl_3$); ^{1}H NMR (400 MHz, $CDCl_3$): δ 7.54 (d, J=8.6 Hz, 2H, Ar), 7.45 (d, J=8.7 Hz, 2H, Ar), 6.86 (d, J=8.8 Hz, 2H, Ar), 7.10 (d, J=8.6 Hz, 2H, Ar), 5.37 (br d, J=3.8 Hz, 1H, 1×olefinic), 4.62 (m, 1H, 1×CHOCO), 4.37 (d, J=7.0 Hz, 1H, CHCl), 3.97 (t, J=6.4 Hz, 2H, 1×OCH_2), 2.31–1.13 (m, 39H, 7×CH, 2×allylic methylene, 14×CH_2), 1.12 (s, 3H, 1×CH_3), 1.01 (s, 3H, 1×CH_3), 0.98 (s, 3H, 1×CH_3), 0.91 (d, J=6.5 Hz, 3H, 1×CH_3), 0.87 (d, J=1.6 Hz, 3H, 1×CH_3), 0.85 (d, J=1.6 Hz, 3H, 1×CH_3), 0.67 (s, 3H, 1×CH_3); ^{13}C NMR (100 MHz, $CDCl_3$): 173.25, 167.73, 159.39, 149.90, 139.77, 133.10, 132.69, 122.65, 121.98, 121.30, 114.92, 114.62, 89.93, 87.03, 73.79, 68.04, 62.60, 56.75, 56.20, 50.09, 42.37, 39.79, 39.57, 39.09, 38.22, 37.05, 36.65, 36.23, 35.83, 34.69, 31.94, 29.02, 28.26, 28.05, 27.88, 25.87, 25.19, 24.99, 23.88, 22.84, 22.59, 21.08, 19.35, 18.76, 16.01, 11.89, 10.90; MS (FAB+): *m/z* calcd for $C_{53}H_{73}ClO_5$: 824.51. Found: 824.94; Anal. Calcd for $C_{53}H_{73}ClO_5$: C, 77.10; H, 8.91. Found: C, 76.88; H, 9.16.

*4.2.12. Cholesteryl 8-[(4-(2-chloro-3-methylpentanoyloxy)-phenylethynyl)-4-phenoxy]octanoate (**TDI-7**)*

R_f=0.42 in 10% EtOAc–hexane; yield: 69%; IR (KBr pellet) ν_{max} in cm^{-1}: 2938, 2216, 1765, 1722, 1606, 1247, 1196, 1164, 780; UV–vis: λ_{max}=311.9 nm, ε=3.12×10^4 L mol^{-1} cm^{-1}; $[\alpha]_D^{22}$ −11.5 (*c* 1.0, $CHCl_3$); ^{1}H NMR (400 MHz, $CDCl_3$): δ 7.53 (d, J=8.7 Hz, 2H, Ar), 7.45 (d, J=8.7 Hz, 2H, Ar), 7.11 (d, J=8.68 Hz, 2H, Ar), 6.86 (d, J=8.8 Hz, 2H, Ar), 5.37 (br d, J=3.5 Hz, 1H, 1×olefinic), 4.60 (m, 1H, 1×CHOCO), 4.3 (d, J=7.0 Hz, 1H, CHCl), 3.97 (t, J=6.3 Hz, 2H, 1×OCH_2), 2.33 −1.05 (m, 43H, 7×CH, 2×allylic methylene, 16×CH_2), 1.13 (s, 3H, 1×CH_3), 1.01 (s, 3H, 1×CH_3), 0.98 (s, 3H, 1×CH_3), 0.92 (d, J=6.4 Hz, 3H, 1×CH_3), 0.87 (d, J=1.6 Hz, 3H, 1×CH_3), 0.85 (d, J=1.6 Hz, 3H, 1×CH_3), 0.67 (s, 3H, 1×CH_3); ^{13}C NMR (100 MHz, $CDCl_3$): 173.17, 167.65, 159.32, 149.83, 139.70, 133.04, 132.62, 122.59, 121.93, 121.24, 114.86, 114.56, 89.88, 86.98, 73.74, 67.99, 62.55, 56.70, 56.16, 50.05, 42.32, 39.74, 39.52, 39.04, 38.17, 37.00, 36.60, 36.19, 35.78, 34.64, 31.89, 28.97, 28.21, 28.00, 27.83, 25.82, 25.15, 24.93, 24.28, 23.83, 22.79, 22.54, 21.03, 19.62, 19.30, 18.71, 15.96, 11.85, 10.85; MS (FAB+): *m/z* calcd for $C_{55}H_{77}ClO_5$: 852.55. Found: 852.65; Anal. Calcd for $C_{55}H_{77}ClO_5$: C, 77.38; H, 9.09. Found: C, 77.45; H, 8.84.

Acknowledgements

We sincerely thank Dr. D.S. Shankar Rao and Dr. S. Krishna Prasad (CLCR) for carrying out X-ray diffraction measurement and helpful discussions.

Supplementary data

Supplementary data associated with this article can be found in the online version, at doi:10.1016/j.tet.2008.02.013.

References and notes

1. (a) Chandrasekhar, S. *Liquid Crystals*, 2nd ed.; Cambridge University: Cambridge and New York, NY, 1992; (b) Tschierske, C. *Annu. Rep. Prog. Chem. Sect. C* **2001**, *97*, 191–267; (c) Kato, T. *Science* **2002**, *295*, 2414–2418.
2. Kitzerow, H. *Chirality in Liquid Crystals*; Kitzerow, H.-S., Bahr, C., Eds.; Springer: New York, NY, 2001.
3. (a) Goodby, J. W.; Nishiyama, I.; Slaney, A. J.; Booth, C. J.; Toyne, K. J. *Liq. Cryst.* **1993**, *14*, 37–66; (b) Goodby, J. W. *Hand Book of Liquid Crystals*; Demus, D., Goodby, J. W., Gray, G. W., Spiess, H.-W., Eds.; Wiley-VCH: Weinheim; New York, NY, 1998; Vol. I, Chapter V, p 115; (c) Goodby, J. W. *Curr. Opin. Colloid Interface Sci.* **2002**, *7*, 326–332.
4. Sage, I. *Liquid Crystals: Applications and Uses*; Bahadur, B., Ed.; World Scientific: Singapore, 1992; Vol. 3, Chapter 20.
5. (a) Lagerwall, S. T. *Ferroelectric and Antiferroelectric Liquid Crystals*; Lagerwall, S. T., Ed.; Wiley-VCH: Weinheim; New York, NY, 1999; (b) Walba, D. M. *Science* **1995**, *270*, 250–251.
6. (a) Garoff, S.; Meyer, R. *Phys. Rev. Lett.* **1977**, *38*, 848–851; (b) Lagerwall, S. T.; Matuszcyk, M.; Rodhe, P.; Odma, L. *The Optics of Thermotropic Liquid Crystals*; Elston, S. J., Sambles, J. R., Eds.; Taylor and Francis: London, 1998; (c) Hartley, C. S.; Kapernaum, N.; Roberts, J. C.; Giesselmann, F.; Lemieux, R. P. *J. Mater. Chem.* **2006**, *16*, 2329–2337.
7. (a) Sakurai, T.; Mikami, N.; Higuchi, R.; Honma, M.; Ozaki, M.; Yoshino, K. *J. Chem. Soc., Chem. Commun.* **1986**, 978–979; (b) Bahr, Ch.; Heppke, G. *Mol. Cryst. Liq. Cryst.* **1987**, *148*, 29–43; (c) Mohr, K.; Kohler, S.; Worm, K.; Pelzl, G.; Diele, S.; Zaschke, H.; Demus, D.; Andersson, G.; Dahl, I.; Lagerwall, S. T.; Skarp, K.; Stebler, B. *Mol. Cryst. Liq. Cryst.* **1987**, *146*, 151–171; (d) Yoshino, K.; Ozaki, M.; Kishino, S.; Sakurai, T.; Mikami, N.; Higuchi, R.; Honma, M. *Mol. Cryst. Liq. Cryst.* **1987**, *144*, 87–103; (e) Twieg, R. J.; Betterton, K.; Nguyen, H. T.; Tang, W.; Hinsberg, W. *Ferroelectrics* **1989**, *91*, 243–265.
8. (a) Zgonik, M.; Rey-Lafon, M.; Destrade, C.; Leon, C.; Nguyen, H. T. *J. Phys. Fr.* **1990**, *51*, 2015–2022; (b) Sierra, T.; Serrano, J. L.; Ross, M. B.; Ezeurra, A.; Zubia, J. *J. Am. Chem. Soc.* **1992**, *114*, 7645–7651.
9. (a) Dierking, I.; Giesselmann, F.; Kußerow, J.; Zugenmaier, P. *Liq. Cryst.* **1994**, *17*, 243–261; (b) Schacht, J.; Dierking, I.; Giesselmann, F.; Mohr, K.; Zaschke, H.; Kuczynski, W.; Zugenmaier, P. *Liq. Cryst.* **1995**, *19*, 151–157.
10. (a) Renn, S. R.; Lubensky, T. C. *Phys. Rev. A* **1988**, *38*, 2132–2147; (b) Slaney, A. J.; Goodby, J. W. *Liq. Cryst.* **1991**, *9*, 849–861; (c) Navailles, I.; Nguyen, H. T.; Barois, P.; Destarde, C.; Isaert, N. *Liq. Cryst.* **1993**, *15*, 479–495.
11. Schacht, J.; Baethge, H.; Giesselmann, F.; Zugenmaier, P. *J. Mater. Chem.* **1998**, *8*, 603–612.
12. Schacht, J.; Zugenmaier, P.; Horii, F. *Liq. Cryst.* **1999**, *26*, 525–533.
13. Thiemann, T.; Vill, V. *J. Phys. Chem. Ref. Data* **1997**, *26*, 291–333.

14. (a) Galatin, A. I.; Novikova, N. S.; Derkach, L. G.; Kramaremko, N. L.; Tsyguleva, O. M.; Kuzin, V. F. *Mol. Cryst. Liq. Cryst.* **1986**, *140*, 11–81; (b) Davis, A. P. *Chem. Soc. Rev.* **1993**, *22*, 243–253; (c) Shinkai, S.; Murata, K. *J. Mater. Chem.* **1998**, *8*, 485–495 and references cited therein; (d) Harwood, S. M.; Toyne, K. J.; Goodby, J. W.; Parsley, M.; Gray, G. W. *Liq. Cryst.* **2000**, *27*, 443–449 and references cited therein.
15. Reinitzer, F. *Monatsh. Chem.* **1888**, *9*, 421–441.
16. (a) Imrie, C. T.; Henderson, P. A. *Curr. Opin. Collidal Interface Sci.* **2002**, *7*, 298–311; (b) Imrie, C. T.; Henderson, P. A. *Chem. Soc. Rev.* **2007**, *36*, 2096–2124 and references cited therein.
17. (a) Yelamaggad, C. V.; Hiremath, U. S.; Shankar Rao, D. S.; Krishna Prasad, S. *Chem. Commun.* **2000**, 57–58; (b) Yelamaggad, C. V.; Anitha Nagamani, S.; Hiremath, U. S.; Shakar Rao, D. S.; Krishan Prasad, S. *Liq. Cryst.* **2002**, *29*, 231–236; (c) Yelamaggad, C. V.; Anitha Nagamani, S.; Hiremath, U. S.; Shakar Rao, D. S.; Krishan Prasad, S. *Mol. Cryst. Liq. Cryst.* **2003**, *397*, 207–229; (d) Yelamaggad, C. V.; Achalkumar, A. S.; Shankar Rao, D. S.; Krishna Prasad, S. *Org. Lett.* **2007**, *9*, 2641–2644.
18. (a) Hardouin, F.; Achard, M. F.; Jin, J.-I.; Shin, J.-W.; Yun, Y.-K. *J. Phys. II* **1994**, *4*, 627–643; (b) Hardouin, F.; Achard, M. F.; Laguerre, M.; Jin, J.-I.; Ko, D.-H. *Liq. Cryst.* **1999**, *26*, 589–599; (c) Yelamaggad, C. V.; Srikrishna, A.; Shankar Rao, D. S.; Krishna Prasad, S. *Liq. Cryst.* **1999**, *26*, 1547–1554; (d) Lee, D. W.; Jin, J.-I.; Laguerra, M.; Achard, M. F.; Hardouin, F. *Liq. Cryst.* **2000**, *27*, 145–152.
19. (a) Yelamaggad, C. V.; Hiremath, U. S.; Shankar Rao, D. S. *Liq. Cryst.* **2001**, *28*, 351–355; (b) Yelamaggad, C. V.; Hiremath, U. S.; Anitha Nagamani, S.; Shankar Rao, D. S.; Krishna Prasad, S. *Liq. Cryst.* **2003**, *30*, 681–690.
20. Lee, J.-W.; Park, Y.; Jin, J.-I.; Achard, M. F.; Hardouin, F. *J. Mater. Chem.* **2003**, *13*, 1367–1372.
21. (a) Tamaoki, N.; Mallia, V. A. *Chem. Mater.* **2003**, *15*, 3237–3239; (b) Kim, K.-N.; Do, E.-D.; Kwon, Y.-W.; Jin, J.-Il. *Liq. Cryst.* **2005**, *32*, 229–237; (c) Lee, W.-K.; Kim, K.-N.; Achard, M. F.; Jin, J.-Il. *J. Mater. Chem.* **2006**, *16*, 2289–2297.
22. (a) Marcelis, A. T. M.; Koudijs, A.; Klop, E. A.; Sudholter, E. J. R. *Liq. Cryst.* **2001**, *28*, 881–887; (b) Yelamaggad, C. V.; Anitha Nagamani, S.; Hiremath, U. S.; Nair, G. G. *Liq. Cryst.* **2001**, *28*, 1009–1015; (c) Yelamaggad, C. V.; Mathews, M. *Liq. Cryst.* **2003**, *30*, 125–133; (d) Marcelis, A. T. M.; Koudijs, A.; Klop, E. A.; Sudholter, E. J. R. *Liq. Cryst.* **2003**, *30*, 1357–1364.
23. (a) Yelamaggad, C. V. *Mol. Cryst. Liq. Cryst.* **1999**, *326*, 149–153; (b) Yelamaggad, C. V.; Hiremath, U. S.; Nair, G. G.; Anitha Nagamani, S. Indian Patent 206282 (148/MAS/2001), 2007; (c) Yelamaggad, C. V.; Anitha Nagamani, S.; Shankar Rao, D. S.; Krishna Prasad, S.; Hiremath, U. S. *Mol. Cryst. Liq. Cryst.* **2001**, *363*, 1–17; (d) Yelamaggad, C. V.; Shashikala, I.; Hiremath, U. S.; Shankar Rao, D. S.; Krishna Prasad, S. *Liq. Cryst.* **2007**, *34*, 153–167; (e) Shankar Rao, D. S.; Krishna Prasad, S.; Raja, V. N.; Yelamaggad, C. V.; Anitha Nagamani, S. *Phys. Rev. Lett.* **2001**, *87*, 085504-1-4; (f) Yelamaggad, C. V.; Mathews, M.; Fujita, T.; Nobuo, I. *Liq. Cryst.* **2003**, *30*, 1079–1087.
24. Cha, S. W.; Jin, J.-I.; Achard, M. F.; Hardouin, F. *Liq. Cryst.* **2002**, *29*, 755–763.
25. Abraham, S.; Mallia, V. A.; Ratheesh, K. A.; Tamaoki, N.; Das, S. *J. Am. Chem. Soc.* **2006**, *128*, 7692–7698.
26. (a) Yelamaggad, C. V.; Achalkumar, A. S.; Bonde, N. L.; Prajapati, A. K. *Chem. Mater.* **2006**, *18*, 1076–1078; (b) Yelamaggad, C. V.; Shashikala, I.; Liao, G.; Shankar Rao, D. S.; Krishna Prasad, S.; Li, Q.; Jakli, A. *Chem. Mater.* **2006**, *18*, 6100–6102; (c) Yelamaggad, C. V.; Bonde, N. L.; Achalkumar, A. S.; Shankar Rao, D. S.; Krishna Prasad, S.; Prajapati, A. K. *Chem. Mater.* **2007**, *19*, 2463–2472.
27. *Hand Book of Liquid Crystals*; Demus, D., Goodby, J. W., Gray, G. W., Spiess, H.-W., Eds.; High Molecular Weight Liquid Crystals; Wiley-VCH: Weinheim; New York, NY, 1998; Vol. 3.
28. Skelton, G.; Dong, D.; Tuffin, R. P.; Kelly, S. M. *J. Mater. Chem.* **2003**, *13*, 450–457.
29. (a) Anana, R.; Rao, P. N.; Chen, Q. H.; Knaus, E. E. *Bioorg. Med. Chem.* **2006**, *14*, 5259–5265; (b) Guillot, M.; Eisler, S.; Weller, K.; Merkle, H. P.; Gallani, J.-L.; Diederich, F. *Org. Biomol. Chem.* **2006**, *4*, 766–769.
30. Koppenhoefer, B.; Schurig, V. *Organic Syntheses*; 1993; Coll. Vol. 8, p 119.
31. Dierking, I. *Textures of Liquid Crystals*; Wiley-VCH GmBH & KGaA: Weinheim, 2003.
32. Goodby, J. W.; Spiess, H.-W. *Ferroelectric Liquid Crystals*; Gordon and Breach Science: Philadelphia, 1991; p 99.
33. (a) Saeva, F. D.; Olin, G. R. *J. Am. Chem. Soc.* **1973**, *95*, 7882–7884; (b) Toriumi, H.; Uematsu, I. *Mol. Cryst. Liq. Cryst.* **1984**, *116*, 21–33; (c) Sisido, M.; Kishi, R. *Macromolecules* **1991**, *24*, 4110–4114; (d) Rout, D. K.; Barman, S. P.; Pulapura, S. K.; Gross, R. A. *Macromolecules* **1994**, *27*, 2945–2950.
34. (a) Yelamaggad, C. V.; Shanker, G. *Liq. Cryst.* **2007**, *34*, 799–809; (b) Yelamaggad, C. V.; Shanker, G. *Liq. Cryst.* **2007**, *34*, 1045–1057.
35. *The Role of Natural Products in Drug Discovery*, 1st ed.; Mulzer, J., Bohlmann, R., Eds.; Springer: Berlin and New York, NY, 2001.
36. Collins, R.; Armitage, J.; Parish, S.; Sleight, P.; Peto, R. *Lancet* **2002**, *360*, 7–22.
37. (a) Woolverton, C. J.; Gustely, E.; Li, L.; Larentovich, O. D. *Liq. Cryst.* **2005**, *32*, 417–423; (b) Seo, S. H.; Twe, G. N.; Chang, J. Y. *Soft Matter.* **2006**, *2*, 886–891; (c) Arnt, L.; Nusslein, K.; Twe, G. N. *J. Polym. Sci., Part A: Polym. Chem.* **2004**, *42*, 3860–3864; (d) Chen, L.; Li, C.-J. *Chem. Commun.* **2004**, 2362–2364.